

# Giant magnetized outflows from the centre of the Milky Way

Ettore Carretti<sup>1</sup>, Roland M. Crocker<sup>2,3</sup>, Lister Staveley-Smith<sup>4,5</sup>, Marijke Haverkorn<sup>6,7</sup>, Cormac Purcell<sup>8</sup>, B. M. Gaensler<sup>8</sup>, Gianni Bernardi<sup>9</sup>, Michael J. Kesteven<sup>10</sup> & Sergio Poppi<sup>11</sup>

**The nucleus of the Milky Way is known to harbour regions of intense star formation activity as well as a supermassive black hole<sup>1</sup>. Recent observations have revealed regions of  $\gamma$ -ray emission reaching far above and below the Galactic Centre (relative to the Galactic plane), the so-called ‘Fermi bubbles’<sup>2</sup>. It is uncertain whether these were generated by nuclear star formation or by quasar-like outbursts of the central black hole<sup>3–6</sup> and no information on the structures’ magnetic field has been reported. Here we report observations of two giant, linearly polarized radio lobes, containing three ridge-like substructures, emanating from the Galactic Centre. The lobes each extend about 60 degrees in the Galactic bulge, closely corresponding to the Fermi bubbles, and are permeated by strong magnetic fields of up to 15 microgauss. We conclude that the radio lobes originate in a biconical, star-formation-driven (rather than black-hole-driven) outflow from the Galaxy’s central 200 parsecs that transports a huge amount of magnetic energy, about  $10^{55}$  ergs, into the Galactic halo. The ridges wind around this outflow and, we suggest, constitute a ‘phonographic’ record of nuclear star formation activity over at least ten million years.**

We use the images of the recently concluded S-band Polarization All Sky Survey (S-PASS) that has mapped the polarized radio emission of the entire southern sky. The survey used the Parkes Radio Telescope at a frequency of 2,307 MHz, with 184 MHz bandwidth, and 9’ angular resolution<sup>7</sup>.

The lobes we report here exhibit diffuse polarized emission (Fig. 1), an integrated total intensity flux of 21 kJy, and a high polarization fraction of 25%. They trace the Fermi bubbles excepting the top western (that is, right) corners where they extend beyond the region covered by the  $\gamma$ -ray emission structure. Depolarization by H II regions establishes that the lobes are almost certainly associated with the Galactic Centre (Fig. 2 and Supplementary Information), implying that their height is  $\sim 8$  kpc. Archival data of WMAP<sup>8</sup> reveal the same structures at a microwave frequency of 23 GHz (Fig. 3). The 2.3–23 GHz spectral index  $\alpha$  (with flux density  $S$  at frequency  $\nu$  modelled as  $S_\nu \propto \nu^\alpha$ ) of linearly polarized emission interior to the lobes spans the range  $-1.0$  to  $-1.2$ , generally steepening with projected distance from the Galactic plane (see Supplementary Information). Along with the high polarization fraction, this phenomenology indicates that the lobes are due to cosmic-ray electrons, transported from the plane, synchrotron-radiating in a partly ordered magnetic field.

Three distinct emission ridges that all curve towards Galactic west with increasing Galactic latitude are visible within the lobes (Fig. 1); two other substructures proceeding roughly northwest and southwest from around the Galactic Centre hint at limb brightening in the biconical base of the lobes. These substructures all have counterparts in WMAP polarization maps (Fig. 3), and one of them<sup>9</sup>, already known

from radio continuum data as the Galactic Centre spur<sup>10</sup>, appears to connect back to the Galactic Centre; we label the other substructures the northern and southern ridges. The ridges’ magnetic field directions (Fig. 3) curve, following their structures. The Galactic Centre spur and southern ridges also seem to have GeV  $\gamma$ -ray counterparts (Fig. 2; also compare ref. 3). The two limb brightening spurs at the biconical lobe base are also visible in the WMAP map, where they appear to connect back to the Galactic Centre area. A possible third spur develops northeast from the Galactic Centre. These limb brightening spurs are also obvious in the Stokes U map as an X-shaped structure centred at the Galactic Centre (Supplementary Fig. 3).

Such coincident, non-thermal radio, microwave and  $\gamma$ -ray emission indicates the presence of a non-thermal electron population covering at least the energy range 1–100 GeV (Fig. 4) that is simultaneously synchrotron-radiating at radio and microwave frequencies and upscattering ambient radiation into  $\gamma$ -rays by the inverse Compton process. The widths of the ridges are remarkably constant at  $\sim 300$  pc over their lengths. The ridges have polarization fractions of 25–31% (see Supplementary Information), similar to the average over the lobes. Given this emission and the stated polarization fractions, we infer magnetic field intensities of 6–12  $\mu$ G for the lobes and 13–15  $\mu$ G for the ridges (see Figs 2 and 3, and Supplementary Information).

An important question about the Fermi bubbles is whether they are ultimately powered by star formation or by activity of the Galaxy’s central, supermassive black hole. Despite their very large extent, the  $\gamma$ -ray bubbles and the X-shaped polarized microwave and X-ray structures tracing their limb-brightened base<sup>11</sup> have a narrow waist of only 100–200 pc diameter at the Galactic Centre. This matches the extent of the star-forming molecular gas ring (of  $\sim 3 \times 10^7$  solar masses) recently demonstrated to occupy the region<sup>12</sup>. With 5–10% of the Galaxy’s molecular gas content<sup>1</sup>, star-formation activity in this ‘central molecular zone’ is intense, accelerating a distinct cosmic ray population<sup>13,14</sup> and driving an outflow<sup>11,15</sup> of hot, thermal plasma, cosmic rays and ‘frozen-in’ magnetic field lines<sup>6,14,16</sup>.

One consequence of the region’s outflow is that the cosmic ray electrons accelerated there (dominantly energized by supernovae) are advected away before they lose much energy radiatively *in situ*<sup>14,16,17</sup>. This is revealed by the fact that the radio continuum flux on scales up to 800 pc around the Galactic Centre is in anomalous deficit with respect to the expectation afforded by the empirical far-infrared/radio continuum correlation<sup>18</sup>. The total 2.3 GHz radio continuum flux from the lobes of  $\sim 21$  kJy, however, saturates this correlation as normalized to the 60  $\mu$ m flux (2 MJy) of the inner  $\sim 160$  pc diameter region (ref. 19). Together with the morphological evidence, this strongly indicates that the lobes are illuminated by cosmic ray electrons accelerated in association with star formation within this region

<sup>1</sup>CSIRO Astronomy and Space Science, PO Box 276, Parkes, New South Wales 2870, Australia. <sup>2</sup>Max-Planck-Institut für Kernphysik, PO Box 103980, 69029 Heidelberg, Germany. <sup>3</sup>Research School of Astronomy and Astrophysics, Australian National University, Weston Creek, Australian Capital Territory 2611, Australia. <sup>4</sup>International Centre for Radio Astronomy Research, M468, University of Western Australia, Crawley, Western Australia 6009, Australia. <sup>5</sup>ARC Centre of Excellence for All-sky Astrophysics (CAASTRO), M468, University of Western Australia, 35 Stirling Highway, Crawley, Western Australia 6009, Australia. <sup>6</sup>Department of Astrophysics/IMAPP, Radboud University Nijmegen, PO Box 9010, 6500 GL Nijmegen, The Netherlands. <sup>7</sup>Leiden Observatory, Leiden University, PO Box 9513, 2300 RA Leiden, The Netherlands. <sup>8</sup>Sydney Institute for Astronomy, School of Physics, The University of Sydney, New South Wales 2006, Australia. <sup>9</sup>Harvard-Smithsonian Center for Astrophysics, 60 Garden Street, Cambridge, Massachusetts 02138, USA. <sup>10</sup>CSIRO Astronomy and Space Science, PO Box 76, Epping, New South Wales 1710, Australia. <sup>11</sup>INAF Osservatorio Astronomico di Cagliari, Strada 54 Località Poggia dei Pini, I-09012 Capoterra (CA), Italy.

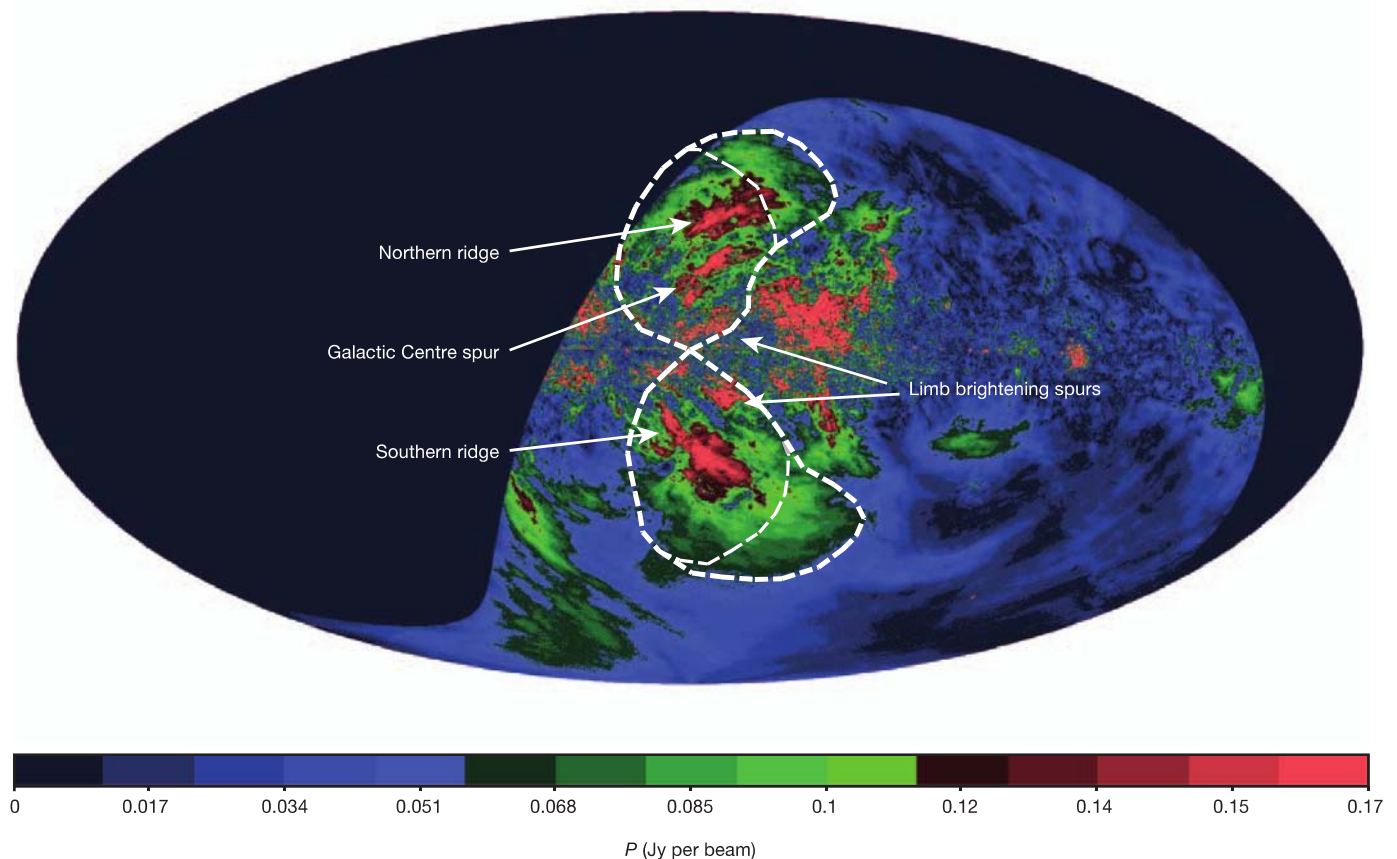


**Figure 1 | Linearly polarized intensity  $P$  at 2.3 GHz from S-PASS.** The thick dashed lines delineate the radio lobes reported in this Letter, while the thin dashed lines delimit the  $\gamma$ -ray Fermi bubbles<sup>2</sup>. The map is in Galactic coordinates, centred at the Galactic Centre with Galactic east to the left and Galactic north up; the Galactic plane runs horizontally across the centre of the map. The linearly polarized intensity flux density  $P$  (a function of the Stokes parameters  $Q$  and  $U$ ,  $P \equiv \sqrt{Q^2 + U^2}$ ) is indicated by the colour scale, and given in units of Jy per beam with a beam size of  $10.75'$  ( $1 \text{ Jy} \equiv 10^{-26} \text{ W m}^{-2} \text{ Hz}^{-1}$ ). The lobes' edges follow the  $\gamma$ -ray border up to Galactic latitude  $b \approx |30|^\circ$ , from which the radio emission extends. The three polarized radio ridges discussed in the text are also indicated, along with the two limb brightening spurs. The

ridges appear to be the front side of a continuous winding of collimated structures around the general biconical outflow of the lobes (see text). The Galactic Centre spur is nearly vertical at low latitude, possibly explained by a projection effect if it is mostly at the front of the northern lobe. At its higher latitudes, the Galactic Centre spur becomes roughly parallel with the northern ridge (above), which itself exhibits little curvature; this is consistent with the overall outflows becoming cylindrical above 4–5 kpc as previously suggested<sup>11</sup>. In such a geometry, synchrotron emission from the rear side of each cone is attenuated by a factor  $\geq 2$  with respect to the front side, rendering it difficult to detect the former against the foreground of the latter and of the Galactic plane (see Supplementary Information).

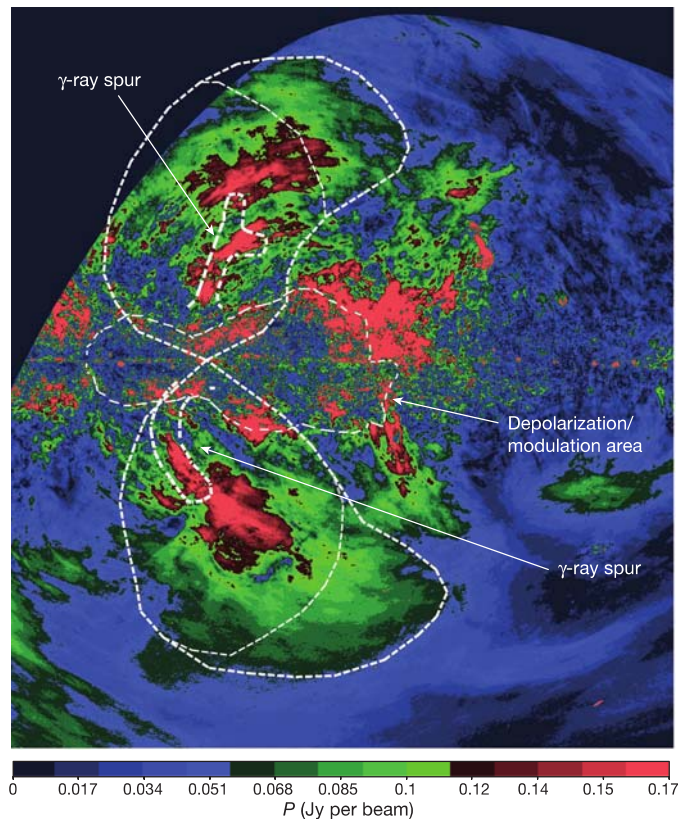
(see Supplementary Information), and that the lobes are not a result of black hole activity.

The ridges appear to be continuous windings of individual, collimated structures around a general biconical outflow out of the Galactic Centre. The sense of Galactic rotation (clockwise as seen from Galactic north) and angular-momentum conservation mean that the ridges get 'wound up'<sup>20</sup> in the outflow with increasing distance from the plane, explaining the projected curvature of the visible, front-side of the ridges towards Galactic west. Polarized, rear-side emission is attenuated, rendering it difficult to detect against the stronger emission from the lobes' front-side and the Galactic plane (Fig. 1 and Supplementary Information).

For cosmic ray electrons synchrotron-emitting at 2.3 GHz to be able to ascend to the top of the northern ridge at  $\sim 7$  kpc in the time it takes them to cool (mostly via synchrotron emission itself) requires vertical transport speeds of  $> 500 \text{ km s}^{-1}$  (for a field of  $15 \mu\text{G}$ ; see Fig. 4). Given the geometry of the Galactic Centre spur, the outflowing plasma is moving at  $1,000\text{--}1,100 \text{ km s}^{-1}$  (Fig. 4 and Supplementary Information), somewhat faster than the  $\sim 900 \text{ km s}^{-1}$  gravitational escape velocity from the Galactic Centre region<sup>21</sup>, implying that 2.3-GHz-radiating electrons can, indeed, be advected to the top of the ridges before they lose all their energy.

Given the calculated fields and the speed of the outflow, the total magnetic energy for each of the ridges,  $(4\text{--}9) \times 10^{52} \text{ erg}$  (see Supplementary Information), is injected at a rate of  $\sim 10^{39} \text{ erg s}^{-1}$  over a few million years; this is very close to the rate at which independent modelling<sup>6</sup> suggests Galactic Centre star formation is injecting magnetic energy into the region's outflow. On the basis of the ridges' individual energetics, geometry, outflow velocity, timescales and plasma content (see Supplementary Information), we suggest that their footpoints are energized by and rotate with the super-stellar clusters inhabiting<sup>1</sup> the inner  $\sim 100 \text{ pc}$  (in radius) of the Galaxy. In fact, we suggest that the ridges constitute 'phonographic' recordings of the past  $\sim 10 \text{ Myr}$  of Galactic Centre star formation. Given its morphology, the Galactic Centre spur probably still has an active footprint. In contrast, the northern and southern ridges seem not to connect to the plane at 2.3 GHz. This may indicate their footpoints are no longer active, though the southern ridge may be connected to the plane by a  $\gamma$ -ray counterpart (see Fig. 2). Unfortunately, present data do not allow us to trace the Galactic Centre spur all the way down to the plane: but a connection is plausible between this structure and one (or some combination) of the  $\sim 1^\circ$ -scale radio continuum spurs<sup>15,22</sup> emanating north of the star-forming giant molecular cloud complexes Sagittarius B and C; a connection is also plausible with the bright,





non-thermal 'radio arc'<sup>1</sup> (itself longitudinally coincident with the  $\sim 4$ -Myr-old Quintuplet<sup>23</sup> stellar cluster).

The magnetic energy content of both lobes is much larger than the ridges,  $(1-3) \times 10^{55}$  erg. This suggests the magnetic fields of the lobes are the result of the accumulation of a number of star formation episodes. Alternatively, if the lobes' field structure were formed over the same timescale as the ridges, it would have to be associated with

**Figure 2 | Lobes' polarized intensity and  $\gamma$ -ray spurs.** Schematic rendering of the edges of two  $\gamma$ -ray substructures evident in the 2–5 GeV Fermi data as displayed in figure 2 of ref. 2, which seem to be counterparts of the Galactic Centre spur and the southern ridge. The map is in Galactic coordinates, with Galactic east to the left and Galactic north up; the Galactic plane runs horizontally across the centre of the map approximately. The linearly polarized intensity flux density  $P$  is indicated by the colour scale, and given in units of Jy per beam with a beam size of  $10.75'$ . The latter appears to be connected to the Galactic Centre by its  $\gamma$ -ray counterpart. With the flux densities and polarization fraction quoted in the text, we can infer equipartition<sup>26</sup> magnetic field intensities of  $B_{\text{eq}} \approx 6 \mu\text{G}$  ( $1 \mu\text{G} \equiv 10^{-10}$  T) if the synchrotron-emitting electrons occupy the entire volume of the lobes, or  $\sim 12 \mu\text{G}$  if they occupy only a 300-pc-thick skin (the width of the ridges). For the southern ridge,  $B_{\text{eq}} \approx 13 \mu\text{G}$ ; for the Galactic Centre spur,  $B_{\text{eq}} \approx 15 \mu\text{G}$ ; and, for the northern ridge,  $B_{\text{eq}} \approx 14 \mu\text{G}$ . Note the large area of depolarization and small-angular-scale signal modulation visible across the Galactic plane extending up to  $|b| \approx 10^\circ$  on either side of the Galactic Centre (thin dashed line). This depolarization is due to Faraday rotation by a number of shells that match H $\alpha$  emission regions<sup>27</sup>, most of them lying in the Sagittarius arm at distances from the Sun up to 2.5 kpc, and some in the Scutum-Centaurus arm at  $\sim 3.5$  kpc. The small-scale modulation is associated with weaker H $\alpha$  emission encompassing the same H II regions and most probably associated with the same spiral arms. Thus 2.5 kpc constitutes a lower limit to the lobes' near-side distance and places the far side beyond 5.5 kpc from the Sun (compare ref. 9). Along with their direction in the sky, this suggests that the lobes are associated with the Galactic bulge and/or Centre.

recent activity of the supermassive black hole, perhaps occurring in concert with enhanced nuclear star-formation activity<sup>4</sup>.

Our data indicate that the process of gas accretion onto the Galactic nucleus inescapably involves star formation which, in turn, energizes an outflow. This carries away low-angular-momentum gas, cosmic rays and magnetic field lines, and has a number of important consequences. First, the dynamo activity in the Galactic Centre<sup>24</sup>, probably required to generate its strong<sup>17</sup> *in situ* field, requires the continual expulsion of small-scale helical fields to prevent dynamo saturation<sup>25</sup>; the presence of the ridges high in the halo may attest to this process. Second, the lobes and ridges reveal how the very active star formation in the Galactic Centre generates and sustains a strong, large-scale magnetic field structure in the Galactic halo. The effect of this on

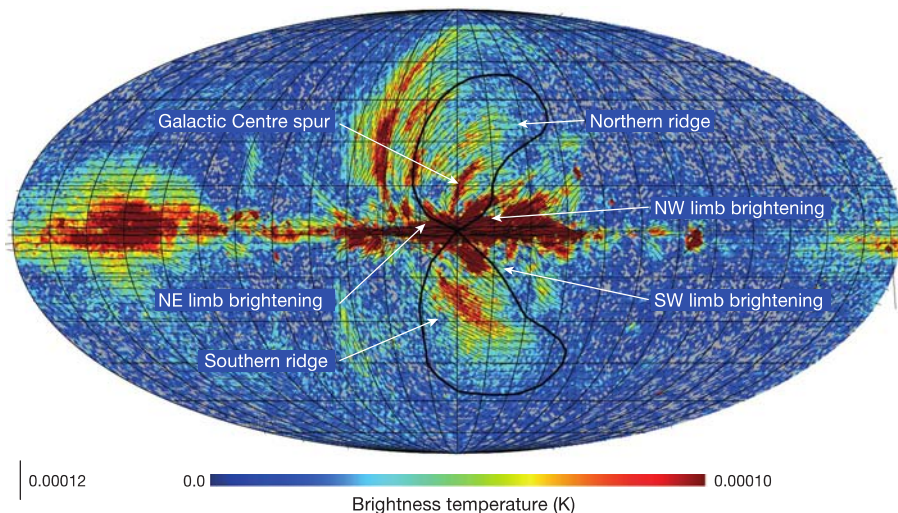


**Figure 3 | Polarized intensity and magnetic angles at 23 GHz from WMAP<sup>8</sup>.** The magnetic angle is orthogonal to the emission polarization angle and traces the magnetic field direction projected on to the plane of the sky (headless vector lines). The three ridges are obvious while traces of the radio lobes are visible (2.3 GHz edges shown by the black solid line). The magnetic field is aligned with the ridges and curves following their shape. Two spurs match the lobe edges northwest and southwest of Galactic Centre and could be limb brightening of the lobes. A third limb brightening spur candidate is also visible northeast of the Galactic Centre. The map is in Galactic coordinates,

centred at the Galactic Centre. Grid lines are spaced by  $15^\circ$ . The emission intensity is plotted as brightness temperature, in K. The vector line length is proportional to the polarized brightness temperature (the scale is shown by the line in the bottom-left corner, in K). Data have been binned in  $1^\circ \times 1^\circ$  pixels to improve the signal-to-noise ratio. From a combined analysis of microwave and  $\gamma$ -ray data (see also Supplementary Information) we can derive the following magnetic field limits (complementary to the equipartition limits reported in the text and Fig. 2): for the overall lobes/bubbles,  $B > 9 \mu\text{G}$ ; and for the Galactic Centre spur,  $11 \mu\text{G} < B < 18 \mu\text{G}$ .

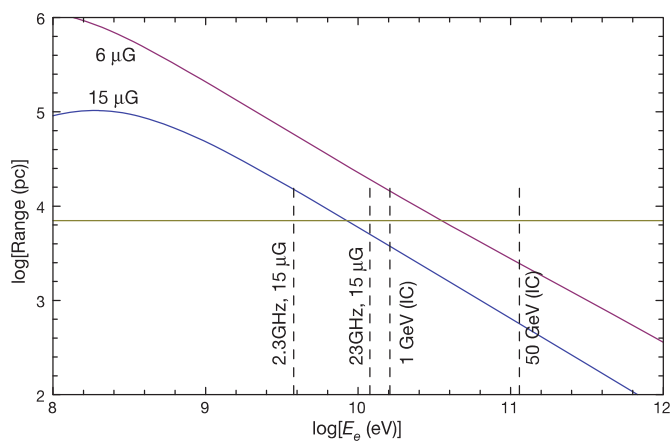


**Figure 4 | The vertical range of cosmic ray electrons as a function of their kinetic energy,  $E_e$ .** Two cases are reported, for field amplitudes of 15 and 6  $\mu\text{G}$  (blue and red curves, respectively). Owing to geometrical uncertainties, adiabatic losses cannot be determined so the plotted range ( $y$  axis) actually constitutes an upper limit. Electrons are taken to be transported with a speed given by the sum of the inferred vertical wind speed ( $1,100 \text{ km s}^{-1}$ ) and the vertical component of the Alfvén velocity in the magnetic field. The former is inferred from the geometry of the northern ridge: if its footpoint has executed roughly half an orbit in the time the Galactic Centre spur has ascended to its total height of  $\sim 4 \text{ kpc}$ , its upward velocity must be close to  $9,100 \text{ km s}^{-1} \times (r/100 \text{ pc})^{-1} \times v_{\text{rot}}/(80 \text{ km s}^{-1})$ , where we have normalized to a footpoint rotation speed of  $80 \text{ km s}^{-1}$  at a radius of 100 pc from the Galactic Centre<sup>12</sup> (detailed analysis gives  $1,100 \text{ km s}^{-1}$ : see Supplementary Information). In a strong, regular magnetic field, the electrons are expected to stream ahead of the gas at the Alfvén velocity<sup>28</sup> in either the ridges ( $B \approx 15 \mu\text{G}$ ,  $v_{\text{A}}^{\text{vert}} \approx 300 \text{ km s}^{-1}$ ; this is a lower limit given that  $n_{\text{H}} \lesssim 0.008 \text{ cm}^{-3}$  on the basis of the ROSAT data<sup>29</sup>) or in the large-scale field of the lobes ( $B \approx 6 \mu\text{G}$ ,  $v_{\text{A}}^{\text{vert}} \gtrsim 100 \text{ km s}^{-1}$  for  $n_{\text{H}} \lesssim 0.004 \text{ cm}^{-3}$  in the lobes' interior as again implied by the data). Also plotted as the vertical dashed lines are the characteristic energies of electrons synchrotron radiating at 2.3 and 23 GHz (for a 15  $\mu\text{G}$  field) and into 1-GeV and 50-GeV  $\gamma$ -rays via inverse Compton ('IC') upscattering of a photon background with characteristic photon energy 1 eV; and the approximate 7 kpc distance of the top of the northern ridge from the Galactic plane.

the propagation of high-energy cosmic rays in the Galactic halo should be considered. Third, the process of gas expulsion in the outflow may explain how the Milky Way's supermassive black hole is kept relatively quiescent<sup>1</sup>, despite sustained, inward movement of gas.

Received 8 August; accepted 26 October 2012.

- Morris, M. & Serabyn, E. The Galactic Centre environment. *Annu. Rev. Astron. Astrophys.* **34**, 645–701 (1996).
- Su, M., Slatyer, T. R. & Finkbeiner, D. P. Giant gamma-ray bubbles from Fermi-LAT: active galactic nucleus activity or bipolar galactic wind? *Astrophys. J.* **724**, 1044–1082 (2010).
- Su, M. & Finkbeiner, D. P. Evidence for gamma-ray jets in the Milky Way. *Astrophys. J.* **753**, 61 (2012).
- Zubovas, K., King, A. R. & Nayakshin, S. The Milky Way's Fermi bubbles: echoes of the last quasar outburst? *Mon. Not. R. Astron. Soc.* **415**, L21–L25 (2011).
- Crocker, R. M. & Aharonian, F. Fermi bubbles: giant, multibillion-year-old reservoirs of Galactic Centre cosmic rays. *Phys. Rev. Lett.* **106**, 101102 (2011).
- Crocker, R. M. Non-thermal insights on mass and energy flows through the Galactic Centre and into the Fermi bubbles. *Mon. Not. R. Astron. Soc.* **423**, 3512–3539 (2012).
- Carretti, E. in *The Dynamic ISM: A Celebration of the Canadian Galactic Plane Survey* (eds Kothes, R., Landecker, T. L. & Willis, A. G.) 276–287 (ASP Conf. Ser. CS-438, Astronomical Society of the Pacific, 2011).
- Hinshaw, G. et al. Five-year Wilkinson Microwave Anisotropy Probe observations: data processing, sky maps, and basic results. *Astrophys. J.* **180** (suppl.), 225–245 (2009).

- Jones, D. I., Crocker, R. M., Reich, W., Ott, J. & Aharonian, F. A. Magnetic substructure in the northern Fermi bubble revealed by polarized microwave emission. *Astrophys. J.* **747**, L12–L15 (2012).
- Sofue, Y., Reich, W. & Reich, P. The Galactic center spur — A jet from the nucleus? *Astrophys. J.* **341**, L47–L49 (1989).
- Bland-Hawthorn, J. & Cohen, M. The large-scale bipolar wind in the Galactic Centre. *Astrophys. J.* **582**, 246–256 (2003).
- Molinari, S. et al. A 100 pc elliptical and twisted ring of cold and dense molecular clouds revealed by Herschel around the Galactic Center. *Astrophys. J.* **735**, L33–L39 (2011).
- Aharonian, F. A. et al. Discovery of very-high-energy  $\gamma$ -rays from the Galactic Centre ridge. *Nature* **439**, 695–698 (2006).
- Crocker, R. M. et al. Wild at heart: the particle astrophysics of the Galactic Centre. *Mon. Not. R. Astron. Soc.* **413**, 763–788 (2011).
- Law, C. J. A multiwavelength view of a mass outflow from the Galactic Center. *Astrophys. J.* **708**, 474–484 (2010).
- Crocker, R. M. et al.  $\gamma$ -rays and the far-infrared-radio continuum correlation reveal a powerful Galactic Centre wind. *Mon. Not. R. Astron. Soc.* **411**, L11–L15 (2011).
- Crocker, R. M., Jones, D. I., Melia, F., Ott, J. & Protheroe, R. J. A lower limit of 50 microgauss for the magnetic field near the Galactic Centre. *Nature* **463**, 65–67 (2010).
- Yun, M. S., Reddy, N. A. & Condon, J. J. Radio properties of infrared-selected galaxies in the IRAS 2 Jy sample. *Astrophys. J.* **554**, 803–822 (2001).
- Launhardt, R., Zylka, R. & Mezger, P. G. The nuclear bulge of the Galaxy III. Large scale physical characteristics of stars and interstellar matter. *Astron. Astrophys.* **384**, 112–139 (2002).
- Heesen, V., Beck, R., Krause, M. & Dettmar, R.-J. Cosmic rays and the magnetic field in the nearby starburst galaxy NGC 253 III. Helical magnetic fields in the nuclear outflow. *Astron. Astrophys.* **535**, A79 (2011).
- Muno, M. P. et al. Diffuse X-ray emission in a deep Chandra image of the Galactic Centre. *Astrophys. J.* **613**, 326–342 (2004).
- Pohl, M., Reich, W. & Schlickeiser, R. Synchrotron modelling of the 400 pc spur at the galactic center. *Astron. Astrophys.* **262**, 441–454 (1992).
- HuBmann, B., Stolte, A., Brandner, W. & Gennaro, M. The present-day mass function of the Quintuplet cluster. *Astron. Astrophys.* **540**, A57 (2012).
- Ferrière, K. Interstellar magnetic fields in the Galactic center region. *Astron. Astrophys.* **505**, 1183–1198 (2009).
- Brandenburg, A. & Subramanian, K. Astrophysical magnetic fields and nonlinear dynamo theory. *Phys. Rep.* **417**, 1–209 (2005).
- Beck, R. & Krause, M. Revised equipartition and minimum energy formula for magnetic field strength estimates from radio synchrotron observations. *Astron. Nachr.* **326**, 414–427 (2005).
- Gaustad, J. E., McCullough, P. R., Rosing, W. & Van Buren, D. A robotic wide-angle H $\alpha$  survey of the southern sky. *Publ. Astron. Soc. Pacif.* **113**, 1326–1348 (2001).
- Kulsrud, R. & Pearce, W. P. The effect of wave-particle interactions on the propagation of cosmic rays. *Astrophys. J.* **156**, 445–469 (1969).
- Almy, R. C. et al. Distance limits on the bright X-ray emission toward the Galactic Center: evidence for a very hot interstellar medium in the galactic X-ray bulge. *Astrophys. J.* **545**, 290–300 (2000).

Supplementary Information is available in the online version of the paper.

**Acknowledgements** This work has been carried out in the framework of the S-band Polarization All Sky Survey collaboration (S-PASS). We thank the Parkes Telescope staff for support, both while setting up the non-standard observing mode and during the observing runs. R.M.C. thanks F. Aharonian, R. Beck, G. Bicknell, D. Jones, C. Law, M. Morris, C. Pfommer, W. Reich, A. Stolte, T. Porter and H. Völk for discussions, and the Max-Planck-Institut für Kernphysik for supporting his research. R.M.C. also acknowledges the support of a Future Fellowship from the Australian Research Council through grant FT110100108. B.M.G. and C.P. acknowledge the support of an Australian Laureate Fellowship from the Australian Research Council through grant FL100100114. M.H. acknowledges the support of research programme 639.042.915, which is partly financed by the Netherlands Organisation for Scientific Research (NWO). The Parkes Radio Telescope is part of the Australia Telescope National Facility, which is funded by the Commonwealth of Australia for operation as a National Facility managed by CSIRO. We acknowledge the use of WMAP data and the HEALPix software package.

**Author Contributions** E.C. performed the S-PASS observations, was the leader of the project, developed and performed the data reduction package, and did the main analysis and interpretation. R.M.C. provided theoretical analysis and interpretation. L.S.-S., M.H. and S.P. performed the S-PASS observations. M.J.K. performed the telescope special set-up that allowed the survey execution. L.S.-S., M.H., B.M.G., G.B., M.J.K. and S.P. were co-proposers and contributed to the definition of the project. C.P. performed the estimate of the H $\alpha$  depolarizing region distance. E.C. and R.M.C. wrote the paper together. All the authors discussed the results and commented on the manuscript.

**Author Information** Reprints and permissions information is available at [www.nature.com/reprints](http://www.nature.com/reprints). The authors declare no competing financial interests. Readers are welcome to comment on the online version of the paper. Correspondence and requests for materials should be addressed to E.C. (Ettore.Carretti@csiro.au).